

Thermoelectric power of TiS_2

A. Amara, Y. Frongillo, M. J. Aubin, and S. Jandl

*Groupe de Recherche sur les Semiconducteurs et les Diélectriques, Département de Physique,
Université de Sherbrooke, Sherbrooke, Québec, Canada J1K 2R1*

J. M. Lopez-Castillo and J. -P. Jay-Gerin

*Groupe du Conseil de Recherches Médicales du Canada en Sciences des Radiations, Département de Médecine Nucléaire
et de Radiobiologie, Université de Sherbrooke, Sherbrooke, Québec, Canada J1H 5N4*

(Received 6 April 1987)

We report on thermoelectric power measurements of TiS_2 taken as a function of temperature. These were done on single crystals between 10 and 300 K and confirm previous conclusions, namely the dominance of ionized-impurity scattering at low temperature and acoustic-phonon scattering at higher temperatures. Exploiting the known T^2 behavior of the resistivity, an effective scattering parameter is calculated and a good fit of the thermoelectric power as a function of temperature is obtained. The variation of thermoelectric power with temperature and the variation with carrier concentration are in excellent agreement since they both give an effective mass of $2.9m$.

I. INTRODUCTION

The layered transition-metal dichalcogenides have been the object of a large number of publications over the years and continue to interest workers in the field. Unusual properties and controversies account for some of this activity. For example, the diselenide TiSe_2 displays a charge-density-wave- (CDW) type transition which leads to unusual thermoelectric power and resistivity behavior as a function of temperature.¹ The related compound TiS_2 which is discussed here has been reported to be a semimetal by some^{2,3} and an extrinsic semiconductor by others.⁴⁻⁸ It should be noted that the earlier references favored the semimetallic model as supported by the apparently metallic behavior of TiS_2 . The more recent investigations however have accumulated enough evidence to present a strong case for the semiconducting model. The reader is referred to the above-mentioned papers for this evidence. On the other hand, even the earlier band-structure calculations⁹⁻¹³ predicted a band gap between the S-based valence p band at Γ and the Ti-based conduction band at L , whereas one recent calculation¹⁴ has yielded a small overlap between these bands. The authors of the latter recognize however that a band shift of their model is necessary to obtain a quantitative agreement with experiment. A convincing result for a value of the indirect band gap was obtained by transport measurements under pressure which at 40 kbar reveal a semiconductor-to-semimetal transition.¹⁵ At ambient pressure, the band gap was found to be 0.18 eV. Nevertheless, a large number of conduction electrons is usually found in TiS_2 . These arise due to the nonstoichiometry of the compound which may be expressed as $\text{Ti}_{1+x}\text{S}_2$. The excess Ti atoms occupy interlayer sites with all four valence electrons becoming delocalized.¹⁶ Even with stoichiometric material, defects may arise as Ti atoms choose to occupy interstitial rather than lattice sites. In what follows, we generally asso-

ciate samples with high carrier concentration ($> 10^{21} \text{ cm}^{-3}$) with a poor stoichiometry.

The unusual behavior of the resistivity as a function of temperature for this material led to an increased interest. A T^2 dependence was reported, which led Thompson¹⁷ to speculate that this was possibly the first observation of electron-electron scattering in a semimetal above room temperature. However, TiS_2 was found to be a semiconductor and the T^2 dependence found to be a special case depending on the stoichiometry. The temperature dependence was found to vary as T^y from 100 to 700 K with y varying from 1.85 for nonstoichiometric samples to 2.2 for stoichiometric samples.^{8,18} Below 40 K, the resistivity varies as T^3 regardless of the stoichiometry.⁸ Thus electron-electron scattering had to be discarded since, furthermore, the large pressure dependence of the resistivity is incompatible with this type of scattering.¹⁹ Rather, this behavior suggests scattering by phonons. Investigating the matter further, Kukkonen *et al.*⁸ examined several modes of scattering only to conclude that none of the considered ones can explain the observed behavior. Klipstein *et al.*,¹⁸ on the other hand, suggest that one possibility would be inter-pocket scattering involving phonon wave vectors near the Brillouin-zone boundary. This is compatible with the interpretation of Koyano *et al.*²⁰ who recently reported the first measurements of the thermoelectric power of TiS_2 as a function of temperature. They added that phonon drag provides an important contribution to the thermoelectric power.

The band-structure calculations of Isomaki *et al.*¹³ predict a TiS_2 Fermi surface composed of three full ellipsoids separated into 12 segments at the 12 L points of the Brillouin zone. The effective-mass components parallel and perpendicular to the layers are calculated to be $m_{\parallel} = 10m$ and $m_{\perp} = 0.40m$ where m represents the free-electron mass. It is convenient to define the anisotropy ratio $\alpha = (m_{\parallel}/m_{\perp})^{1/2}$ which for the above result is

5. As a comparison, Inoue *et al.*²¹ had to use a value of $\alpha=11$ to fit their calculated resistivity due to impurity scattering of Ti^{4+} ions at 0 K to their experimental residual resistivity ρ_1^0 as a function of carrier density. To pursue our comparisons of various data, we recall the definition of the density of states effective mass $m^*=(m_\perp^2 m_\parallel)^{1/3}$. Inoue's measurements do not lead to a value for m^* but Isomaki's calculations give $m^*=1.17m$. Combining magnetic susceptibility and Seebeck coefficient results, Thompson¹⁷ claims a value of $m^*/m=1.5$. Kukkonen *et al.*⁸ measured the Seebeck coefficient of TiS_2 single crystals with carrier concentrations ranging from 2.2×10^{20} to $3.4 \times 10^{21} \text{ cm}^{-3}$ at 300 K and report an effective-mass ratio of the order of unity. The validity of these experimental results is questioned below. Very recently, Inoue *et al.*²² reported specific-heat measurements of TiS_2 at low temperature. From the familiar plot of C/T versus T^2 , they obtain an intercept of 2 mJ/mol K^2 from which one may calculate an effective-mass ratio of the order of 5.

This paper attempts to clarify the uncertainty in these effective-mass estimates and will also provide quantitative results for the effective scattering parameter following accurate thermoelectric power measurements of TiS_2 as a function of temperature.

II. THEORY

In this section we will establish the equations which will be invoked for the interpretation of our transport data. The Seebeck coefficient,²³ for a temperature gradient in the x direction, may be written

$$S = \frac{1}{eT} \frac{\int d\mathbf{k} (\mathbf{E}_\mathbf{k} - E_F) \tau_\mathbf{k} (\mathbf{v}_\mathbf{k})_x^2 \left[-\frac{\partial f_0(E_\mathbf{k})}{\partial E_\mathbf{k}} \right]}{\int d\mathbf{k} \tau_\mathbf{k} (\mathbf{v}_\mathbf{k})_x^2 \frac{-\partial f_0(E_\mathbf{k})}{\partial E_\mathbf{k}}}, \quad (1)$$

where $(\mathbf{v}_\mathbf{k})_x$ is the x component of the velocity in \mathbf{k} space, f_0 is the equilibrium Fermi-Dirac distribution function, and e is the electronic charge. $(\mathbf{E}_\mathbf{k} - E_F)$ represents an energy above the Fermi energy E_F and the relaxation time $\tau_\mathbf{k}$ is given²⁴ by the usual formula for semiconductors

$$\tau_\mathbf{k} = \tau_0(T) \left(\frac{E_\mathbf{k}}{E_F} \right)^p.$$

The scattering parameter p will be discussed later. Assuming a parabolic conduction band, Eq. (1) may be shown to give the same result for spherical and ellipsoidal constant-energy surfaces, namely

$$S = \frac{k_B}{e} \left[\frac{(p + \frac{5}{2}) \Gamma(p + \frac{5}{2}) F_{p+3/2}(\xi)}{(p + \frac{3}{2}) \Gamma(p + \frac{3}{2}) F_{p+1/2}(\xi)} - \xi \right], \quad (2)$$

where

$$F_j(\xi) = \frac{1}{\Gamma(j+1)} \int_0^\infty \frac{x^j dx}{1 + e^{x-\xi}},$$

and $\xi = E_F/k_B T$. In most of the relevant temperature

range, TiS_2 samples are degenerate and Eq. (2) becomes

$$S = \frac{k_B}{e} \frac{\pi^2}{3\xi} \left(p + \frac{3}{2} \right). \quad (3)$$

Recalling the ellipsoidal nature of the Fermi surface, which consists of three equivalent electron pockets, one may show that the transverse component of the Fermi wave vector $k_{F\perp}$ is related to the carrier concentration N by

$$k_{F\perp} = \left[\frac{\pi^2}{\alpha} N \right]^{1/3},$$

so that

$$E_F = \frac{\hbar^2}{2m_\perp} \left[\frac{\pi^2}{\alpha} N \right]^{2/3} = \frac{\hbar^2}{2m^*} (\pi^2 N)^{2/3}, \quad (4)$$

and

$$S = \frac{2k_B^2 \pi^{2/3}}{3e \hbar^2} m^* T \left(p + \frac{3}{2} \right) N^{-2/3}. \quad (5)$$

The Seebeck coefficient thus varies linearly with temperature as is well known for degenerate semiconductors. It is also proportional to $N^{-2/3}$, a fact verified by several workers for TiS_2 including Kukkonen *et al.*⁸ Unfortunately, they analyzed their data on the basis of a value of $p = \frac{3}{2}$ for phonon scattering. (The proper values are $-\frac{1}{2}$ for acoustic phonon scattering and $\frac{3}{2}$ for ionized impurity scattering.) Thus their estimate of m^* should be revised.

Usually, more than one scattering mechanism is present at one time and the scattering parameter p takes on an effective value p^* . It is important to make a distinction between the manner in which one takes into account more than one scattering mechanism and more than one type of carrier. Koyano *et al.*²⁰ did not make this distinction. If one assumes two types of scattering, p^* may be calculated in the following way:

$$\frac{1}{\tau(E_\mathbf{k})} = \frac{1}{\tau_p(E_\mathbf{k})} + \frac{1}{\tau_i(E_\mathbf{k})},$$

where

$$\tau_n(E_\mathbf{k}) = \tau_{0n} \left(\frac{E_\mathbf{k}}{E_F} \right)^{p_n},$$

and $n=p, i$ for acoustic-phonon and ionized-impurity scattering, respectively. One can show using the Sommerfeld expansion²⁵ for the degenerate case that

$$p^* = \left[\frac{\tau_{0i}}{\tau_{0i} + \tau_{0p}} \right]^{p_p} + \left[\frac{\tau_{0p}}{\tau_{0p} + \tau_{0i}} \right]^{p_i}. \quad (6)$$

Like τ_{0p} , p^* is a function of temperature. Since $p_p = -\frac{1}{2}$ and $p_i = \frac{3}{2}$, one can simplify this equation by defining $r = \tau_{0p}/\tau_{0i}$ so that

$$p^* = \frac{1}{2} \left[\frac{3r-1}{r+1} \right].$$

Equation (5) also shows the Seebeck coefficient to be proportional to $(p+d)$ with $d = \frac{3}{2}$ for spherical or ellipsoidal Fermi surfaces. In the case of cylindrical Fermi surfaces, $d = 1$. Table I summarizes the $(p+d)$ values for various cases including neutral impurity scattering in addition to the other mechanisms already mentioned.

III. EXPERIMENTAL PROCEDURE

Good-quality single crystals of TiS_2 were obtained by iodine transport in quartz ampoules. They grew in the form of thin shiny platelets of approximately $\frac{1}{2} \text{ cm}^2$ by $100\text{-}\mu\text{m}$ thick. Two successful growth runs were performed at different temperature conditions, giving samples of different carrier concentrations as expected, since stoichiometry depends on these conditions. One sample of $5 \times 1 \text{ mm}^2$ was cut from a platelet obtained from each run.

The thermoelectric power measurements were performed from 10 to 300 K using a dynamical method to avoid stray voltages, as previously described,²⁶ except that the present system is completely automated. The computer program requires that the plot of thermo-emf versus temperature difference produce a straight line with a coefficient of correlation greater than 0.99 before accepting a datapoint. In practice, it is greater than 0.995. Excellent data can thus be obtained as one can judge from the absence of any apparent scatter in the experimental points.

IV. RESULTS AND DISCUSSION

The results obtained from two samples of TiS_2 are illustrated in Fig. 1, which show the Seebeck coefficient as a function of temperature. The curves extrapolate to the origin as expected but display a marked change in slope at $\sim 50 \text{ K}$. Recalling Eq. (5), the Seebeck coefficient is proportional to $p+d$. Since the dominant scattering mechanism and consequently p^* is supposed to vary with temperature, the change in slope is not unexpected. More specifically, the slope decreases by a factor ~ 3 for both samples as the temperature increases. Consulting Table I, we find that only one case is compatible with this result, namely ionized impurity scattering at low temperature and acoustic phonon scattering at room temperature for ellipsoidal Fermi surfaces. Such a result is most gratifying, since it confirms previous conclusions obtained from altogether different techniques.^{15,18}

One may pursue the matter further in order to evaluate the value of p^* as a function of temperature. We

TABLE I. Scattering parameter $p+d$ under various conditions.

	p	$p+d$ (ellipsoidal)	$p+d$ (cylindrical)
Ionized impurity	$\frac{3}{2}$	3	$\frac{5}{2}$
Neutral impurity	0	$\frac{3}{2}$	1
Acoustic phonons	$-\frac{1}{2}$	1	$\frac{1}{2}$
Optical phonons	$\frac{1}{2}$	2	$\frac{3}{2}$

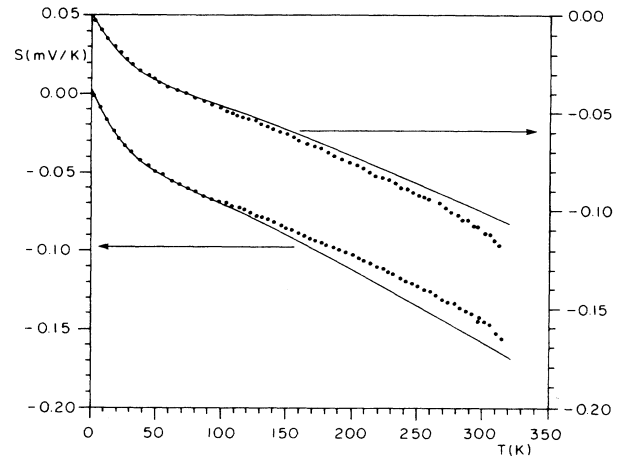


FIG. 1. Thermoelectric power of samples 1 and 2 as a function of temperature. For clarity, the ordinate axis and scale are different for the two samples. The curves are the result of the fitting procedure described in the text.

note that the scattering mechanisms have been identified and correspond to those assumed in Eq. (6). In this equation we can say that τ_{0i} is independent of temperature and that τ_{0p} is inversely proportional to the square of the temperature ($\tau_{0p} = A/T^2$) in general agreement with the resistivity data described in the Introduction. Thus

$$r = \frac{A}{T^2 \tau_{0i}} = \frac{r_0}{T^2},$$

where r_0 is independent of temperature. Equation (3) may then be rewritten

$$S = \frac{k_B^2 \pi^2 T}{3eE_F} \left[\frac{1}{2} \left[\frac{3r-1}{r+1} \right] + \frac{3}{2} \right]$$

$$= \frac{k_B^2 \pi^2 T}{3eE_F} \left[\frac{3r_0 + T^2}{r_0 + T^2} \right],$$

where p has been replaced by p^* . The above expressions

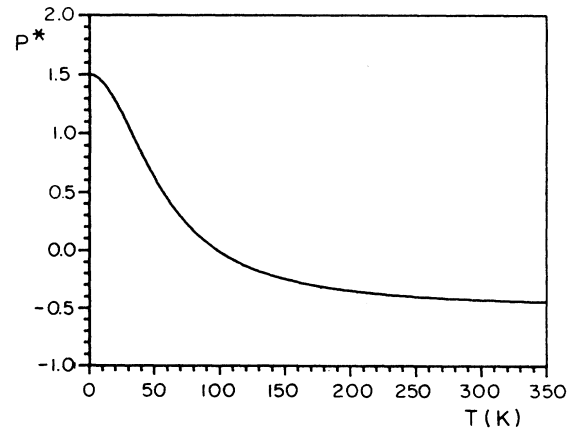


FIG. 2. Effective scattering parameter p^* as a function of temperature.

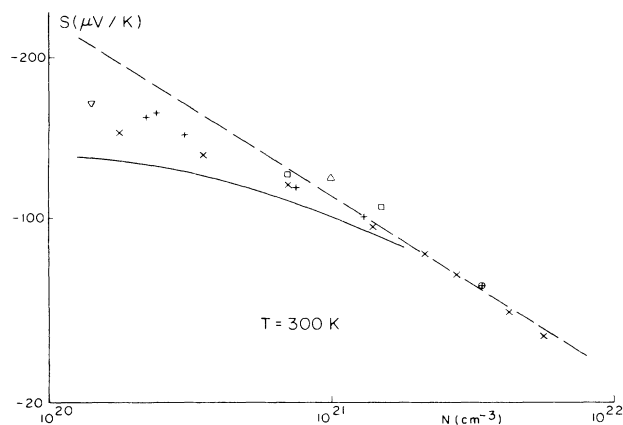


FIG. 3. Thermoelectric power of TiS_2 as a function of carrier concentration (logarithmic scale) according to various authors. \square , this work; $+$, Ref. 8; ∇ , Ref. 15; \times , Ref. 3; \triangle , Ref. 20; \circ , Ref. 27.

contain only two adjustable parameters which are essentially independent of temperature, r_0 , which is defined as A/τ_{0i} and E_F which must be constant since our measurements show that the Hall coefficient is independent of temperature. Thus a fit of the thermoelectric power as a function of temperature is obtained, yielding values of $r_0 = 3200 \text{ K}^2$, $E_F = 48.7 \text{ meV}$ for $N = 7 \times 10^{20} \text{ cm}^{-3}$ and $r_0 = 2400 \text{ K}^2$, $E_F = 77.4 \text{ meV}$ for $N = 15 \times 10^{20} \text{ cm}^{-3}$. The fit with these values is shown in Fig. 1 and is quite satisfactory. On the other hand, attempts to fit the data with a more traditional $1/T$ variation for τ_{0p} fail dramatically especially in the 50-K region. Combining these values of E_F with those of N obtained from the Hall coefficient in Eq. (4), leads to effective-mass values of $2.84m$ and $2.97m$ for the two samples. Knowledge of r_0 allows one to obtain p^* as a function of temperature (see Fig. 2), indicating more clearly the tendency towards values of $\frac{3}{2}$ and $-\frac{1}{2}$ in the limit of low and high temperatures, respectively.

The variation of the thermoelectric power with carrier concentration will now be reconsidered. Equation (5) predicts a variation proportional to $N^{-2/3}$ which has been verified by Kukkonen *et al.*⁸ but with an incorrect value of p as mentioned above. The room-temperature data available from the literature and our own are included in Fig. 3. Above $5 \times 10^{20} \text{ cm}^{-3}$, S is indeed proportional to $N^{-2/3}$ with a slope which yields the following result for $T = 300 \text{ K}$:

$$(m^*/m)(p^* + \frac{3}{2}) = 3.02.$$

Above, it was found that p^* at room temperature is -0.43 and -0.45 for the two samples so that effective mass ratios of 2.82 and 2.88 are obtained, in excellent agreement with our other result obtained in an independent manner. Finally, the deviation from a straight line behavior in Fig. 3 is simply due to the degeneracy approximation which becomes invalid as N decreases as will now be demonstrated. In order to use the Fermi-Dirac integrals, half integer values of p must be assumed. A value of $-\frac{1}{2}$ will be taken, a reasonable approximation for $T = 300 \text{ K}$ where p^* was found to be -0.44 ± 0.01 . Setting $m^*/m = 2.88$, the average of the four values obtained in this paper, we used Eq. (2) to calculate S yielding the curve in Fig. 3. The curvature is qualitatively correct, the discrepancy being due to the approximation for p^* and to fine detail in the model.

V. CONCLUSION

We have presented the second report of thermoelectric power measurements of TiS_2 as a function of temperature, the first having been presented recently by Koyano *et al.*²⁰ Improvements have been made in the quality of the data and in the analysis through a careful treatment of the case involving more than one scattering mechanism. Furthermore, only two adjustable parameters are necessary to fit these data. In fact, the overall behavior of the thermoelectric power of TiS_2 is successfully described by diffusion processes only, without referring to phonon drag effects, in agreement with the findings of Lopez-Castillo *et al.*²⁸

Finally, the effective mass of conduction electrons in TiS_2 has been determined by two independent methods which yield the same result, namely $2.9m$. This result is much higher than the experimental values quoted in Refs. 8 and 17. In the former, inserting the proper value for p yields an effective-mass ratio of ~ 3 rather than unity. In the latter, one may suspect the results since the same fit produced an unusually low g value (spectroscopic splitting factor). The more recent data of Inoue²² yields an effective mass ratio of ~ 5 which is in accord with our results within experimental error.

ACKNOWLEDGMENT

The authors thank A. Lakhani, now with Bendix Corporation, for his assistance in the early stages of this work.

¹F. J. Di Salvo, D. E. Moncton, and J. V. Waszczak, *Phys. Rev. B* **14**, 4321 (1976).

²S. Takeuchi and H. Katsuda, *J. Jpn. Inst. Met.* **34**, 758 (1970).

³A. H. Thompson, F. R. Gamble, and C. R. Simon, *Mater. Res. Bull.* **10**, 915 (1975).

⁴J. A. Wilson, *Solid State Commun.* **22**, 551 (1977).

⁵R. H. Friend, D. Jerome, W. Y. Liang, J. C. Mikkelsen, and A. D. Yoffe, *J. Phys. C* **10**, L705 (1977).

⁶C. H. Chen, W. Fabian, F. C. Brown, K. C. Woo, B. Davies, B. Delong, and A. H. Thompson, *Phys. Rev. B* **21**, 615 (1980).

⁷E. M. Logothetis, W. J. Kaiser, C. A. Kukkonen, S. P. Faile, R. Colella, and J. Gambold, *J. Phys. C* **12**, L521 (1979).

⁸C. A. Kukkonen, W. J. Kaiser, E. M. Logothetis, B. J. Blumenstock, P. A. Schroeder, S. P. Faile, R. Colella, and J. Gambold, *Phys. Rev. B* **24**, 1691 (1981).

- ⁹R. B. Murray and A. D. Yoffe, *J. Phys. C* **5**, 3038 (1972).
- ¹⁰H. W. Myron and A. Freeman, *Phys. Rev. B* **11**, 2087 (1975).
- ¹¹A. Zunger and A. Freeman, *Phys. Rev. B* **16**, 906 (1977).
- ¹²D. W. Bullett, *J. Phys. C* **11**, 4501 (1978).
- ¹³H. M. Isomaki, J. von Boehm, and P. Krusius, *J. Phys. C* **12**, 3239 (1979).
- ¹⁴G. A. Benesh, A. M. Woolley, and C. J. Umrigar, *J. Phys. C* **18**, 1595 (1985).
- ¹⁵P. C. Klipstein and R. H. Friend, *J. Phys. C* **17**, 2713 (1984).
- ¹⁶J. A. Wilson, *Phys. Status Solidi* **86**, 11 (1978).
- ¹⁷A. H. Thompson, *Phys. Rev. Lett.* **35**, 1786 (1975).
- ¹⁸P. C. Klipstein, A. G. Bagnall, W. Y. Liang, E. A. Marseglia, and R. H. Friend, *J. Phys. C* **14**, 4067 (1981).
- ¹⁹R. H. Friend, D. Jerome, and A. D. Yoffe, *J. Phys. C* **15**, 2183 (1982).
- ²⁰M. Koyano, H. Negishi, Y. Ueda, M. Sasaki, and M. Inoue, *Phys. Status Solidi B* **138**, 357 (1986).
- ²¹M. Inoue, M. Koyano, H. Negishi, Y. Ueda, and H. Sato, *Phys. Status Solidi B* **132**, 295 (1985).
- ²²M. Inoue, Y. Muneta, H. Negishi, and M. Sasaki, *J. Low Temp. Phys.* **63**, 235 (1986).
- ²³F. J. Blatt, *Physics of Electronic Conduction in Solids* (McGraw-Hill, New York, 1968), p. 209.
- ²⁴P. Kiréev, *La Physique des Semiconducteurs* (Editions MIR, Moscow, 1975), p. 465.
- ²⁵N. W. Ashcroft and N. D. Mermin, *Solid State Physics* (Holt, Rinehart, and Winston, New York, 1976), p. 760.
- ²⁶A. A. Lakhani, S. Jandl, C. Ayache, and J. P. Jay-Gerin, *Phys. Rev. B* **28**, 1978 (1983).
- ²⁷Y. Frongillo (unpublished).
- ²⁸J. M. Lopez-Castillo, A. Amara, S. Jandl, J. P. Jay-Gerin, C. Ayache, and M. J. Aubin (unpublished).